Tristan Neumann, Inke Jess, Cesar dos Santos Cunha, Huayna Terraschke and Christian Näther*

Cd(II) and Zn(II) thiocyanate coordination compounds with 3-ethylpyridine: synthesis, crystal structures and properties

https://doi.org/10.1515/znb-2017-0186
Received November 15, 2017; accepted November 29, 2017

Abstract: Reaction of $Cd(NCS)_2$ and $Zn(NCS)_2$ with 3-ethylpyridine leads to the formation of compounds of compositions $M(NCS)_2(3\text{-ethylpyridine})_4$ (M = Cd, **1-Cd**; Zn, **1-Zn**) and $M(NCS)_2(3\text{-ethylpyridine})_2$ (M = Cd, **2-Cd**; Zn, **2-Zn**). **1-Cd** and **1-Zn** are isotypic and form discrete complexes in which the metal cations are octahedrally coordinated by two *trans*-coordinating N-bonded thiocyanate anions and four 3-ethylpyridine co-ligands. In **2-Cd** the cations are also octahedrally coordinated but linked into chains by pairs of μ-1,3-bridging anionic ligands. **2-Zn** is built up of discrete complexes, in which the Zn cation is tetrahedrally coordinated by two N-bonded thiocyanate anions and two 3-ethylpyridine co-ligands. Compounds **1-Cd**, **2-Cd** and **2-Zn** can be prepared in a pure state, whereas **1-Zn** is unstable and transforms on storage into **2-Zn**. If **1-Cd** and **1-Zn** are heated, a transformation into **2-Cd**, respectively **2-Zn** is observed. Luminescence measurements reveal that **1-Cd**, **2-Cd** and **2-Zn** emit light in the blue spectral range with maxima at, respectively, 21724, 21654 and 22055 cm^{-1}, assigned to ligand-based luminescence.

Keywords: 3-ethylpyridine; Cd and Zn coordination compounds; crystal structures; luminescence properties; thermal properties.

1 Introduction

Investigations on the synthesis, crystal structures and properties of new coordination polymers is still an important field in coordination chemistry. One of the major advantages of this class of compounds is the fact, that based on simple considerations concerning the coordination properties of metal cations, anionic ligands and neutral co-ligands, the dimensionality of their coordination networks can be predicted to some extent [1–6]. In this context numerous compounds have been reported that show different physical properties like, e.g. gas sorption, luminescence or magnetism [7–16].

Our interest focuses on coordination compounds and polymers based on 3d transition metal cations and thiocyanate ligands with additional N-donor co-ligands [17–24]. This anionic ligand shows a large variety of coordination modes with the N-terminal and the μ-1,3-bridging mode as the most prominent [25–32]. Compounds with a bridging coordination are of special interest, because magnetic exchange can be mediated [33–39]. Unfortunately, the metal cations in which we are interested like Mn(II), Fe(II), Co(II) and Ni(II) are not very chalcophilic and usually prefer a terminal N-coordination of the anionic ligands and therefore, the synthesis of the desired compounds with a bridging coordination is sometimes difficult to perform. In this case, coordination compounds with terminal thiocyanate anions can be heated, which in most cases leads to a stepwise removal of the co-ligands and the formation of the desired compounds in which the metal cations are linked by μ-1,3-bridging anionic ligands [40, 41]. Following this procedure microcrystalline powders are obtained, that cannot be characterized by single crystal X-ray diffraction. To obtain structural information, similar compounds with Cd(II) can be prepared, since Cd(II) is much more chalcophilic and therefore the bridging compounds are usually more stable than those with a terminal coordination of the anionic ligands. In many cases they are isotypic to the paramagnetic analogs and thus, the structure of the latter can be determined by Rietveld refinements [42]. It is noted, that thermal decomposition of Co(II) compounds sometimes lead to the formation of tetrahedral complexes, which exhibit the same ratio between the metal thiocyanate and the organic co-ligand. Such intermediates can be

***Corresponding author: Christian Näther,** Institut für Anorganische Chemie, Christian-Albrechts-Universität zu Kiel, Max-Eyth-Straße 2, 24118 Kiel, Germany, Fax: +49-431-8801520,
E-mail: cnaether@ac.uni-kiel.de
Tristan Neumann, Inke Jess, Cesar dos Santos Cunha and Huayna Terraschke: Institut für Anorganische Chemie, Christian-Albrechts-Universität zu Kiel, Max-Eyth-Straße 2, 24118 Kiel, Germany

identified by the preparation of corresponding Zn compounds which are usually tetrahedral coordinated [43]. This is the main reason why we are generally interested in the chemical and structural properties of coordination compounds based on Cd(II) and Zn(II) thiocyanate. In this context, it is noted that these compounds frequently show luminescence, and several of them are reported in literature [44–49]. Even if this luminescence is based predominantly on the organic ligands, we became interested in this behavior to check if differences are observed between discrete compounds or coordination polymers or between compounds with different metal cations or terminal or bridging ligands [50–52].

In the course of our systematic investigations we predominantly used pyridine derivatives that are substituted at the 4-position, that, except of Zn(II), mostly form coordination polymers with bridging anionic ligands. We also prepared some compounds where the substituent is directly neighbored to the coordinating N atom. In this case the synthesis of coordination polymers is more difficult and with, e.g. Co(II) discrete complexes were obtained, presumably because of steric reasons [43]. Therefore we used e.g. 3-hydroxymethyl or 3-aminomethylpyridine in previous works, but in most cases compounds were obtained, in which the metal cations are linked *via* the pyridine co-ligand, which prevented the formation of metal thiocyanate chains. To avert such a behavior we became interested in 3-ethylpyridine as a co-ligand, for which no thiocyanate coordination polymers were reported. There are only two polymorphic modifications of $Ni(NCS)_2(3\text{-ethylpyridine})_2$ reported in literature that form discrete complexes, but compounds based on Cd(II) and Zn(II) are unknown [53].

2 Results and discussion

2.1 Synthesis

Preliminary synthetic investigations using different amounts of $Cd(NCS)_2$ or $Zn(NCS)_2$ and 3-ethylpyridine indicated that only four crystalline phases are accessible from solution. If an excess of the co-ligand is used, one Cd and one Zn compound are obtained, that might be isotypic. Elemental analysis indicated a composition that is close to $M(NCS)_2(3\text{-ethylpyridine})_4$ (M = Cd; **1-Cd**, Zn; **1-Zn**). If the reactants are used in a ratio of 1:2, an additional crystalline phase is obtained for each cation in which the ratio between the metal salt and 3-ethylpyridine is 1:2. The two compounds (**2-Cd** and **2-Zn**) are not isotypic and XRPD measurements indicate that most batches of **1-Zn** are contaminated with **2-Zn**. For all compounds suitable single crystals were grown and investigated by X-ray diffraction.

2.2 Crystal structures

Compounds **1-Cd** and **1-Zn** are isotypic and crystallize in the triclinic space group $\bar{P}1$ with one formula unit in the unit cell. The asymmetric unit consists of one metal cation which is located on a center of inversion, and one thiocyanate anion as well as two 3-ethylpyridine ligands that are located in general positions (Fig. 1).

The crystal structures consist of discrete complexes in which the cations are octahedrally coordinated by four 3-ethylpyridine co-ligands and two terminal N-bonded thiocyanate anions (Fig. 1). For **1-Cd** the Cd–N distances are between 2.2990(2) and 2.389(2) Å which is in the usual range observed for such compounds. As expected, in **1-Zn** the Zn–N distances are shortened to values between 2.106(2) and 2.235(1) Å. In both compounds all angles deviate from the ideal values, which shows that the octahedra are slightly distorted.

Compound **2-Cd** also crystallizes in the triclinic space group $\bar{P}1$ and the asymmetric unit consists of one Cd cation, two crystallographically independent thiocyanate anions and two 3-ethylpyridine ligands, all of them being located in general positions (Fig. 2: top). One ethyl group of one co-ligand and a large part of the second co-ligand are disordered and were refined using a split model (see Experimental section). The Cd cations are coordinated by two 3-ethylpyridine ligands as well as two N and two S-bonding thiocyanate anions within slightly distorted octahedra (Fig. 2: top). The Cd–N distances ranges from 2.305(3) to 2.341(3) Å and the Cd–S distances amount to 2.7446(2) and 2.752(2) Å.

The Cd cations are linked by pairs of anionic ligands into linear chains in which the thiocyanate N and S atoms as well as the 3-ethylpyridine N atoms are always in *trans*-arrangement. This is a very common motif in this family of compounds (Fig. 2: bottom). Within these chains the 6-membered rings of the co-ligands are alternatingly rotated out of the chain vector, which can be traced back to steric repulsion between the co-ligands (Fig. 2: bottom). The intrachain Cd–Cd distance amounts to 5.875 Å and the shortest interchain Cd–Cd distance is 9.755 Å.

Compound **2-Zn** crystallizes in the monoclinic space group $P2_1/m$ with the Zn cations located on a crystallographic mirror plane. The lattice parameters are close

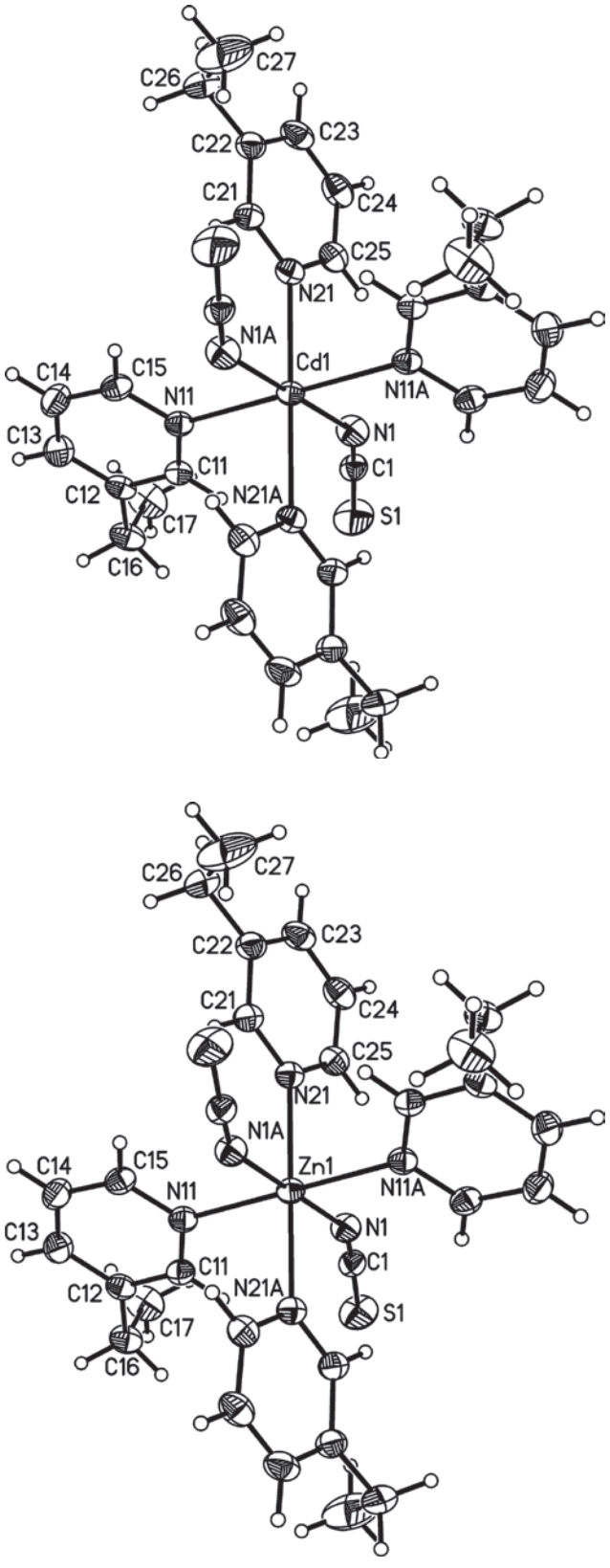

Fig. 1: Molecular structures of **1-Cd** (top) and **1-Zn** (bottom) with labeling and displacement ellipsoids drawn at 50% probability level. Symmetry codes: A = –*x*+1, –*y*+1, –*z*+1.

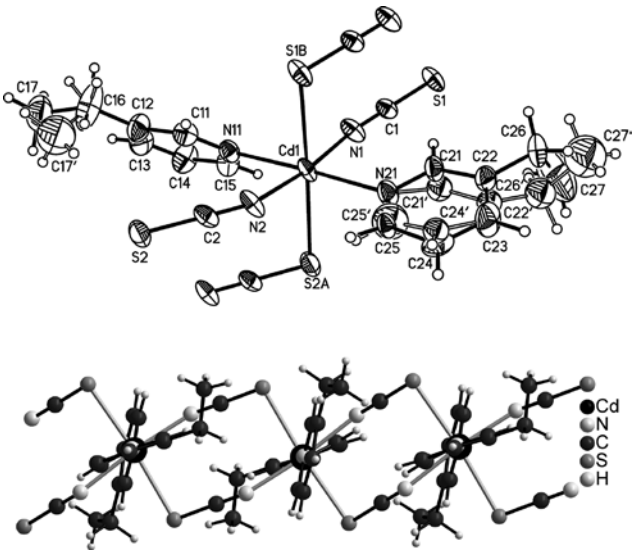

Fig. 2: Crystal structure of **2-Cd** with labeling and displacement ellipsoids drawn at the 50% probability level. Disordering of the 3-ethylpyridine ligand is shown as full and open bonds (top), and view of a single chain is presented (bottom). Symmetry codes: A = –*x*, –*y*+1, –*z*+1. In the bottom figure the disorder is not shown.

to that for orthorhombic but the crystal symmetry is clearly 2/*m*. Consequently, the crystals are twinned and therefore, a twin-refinement was performed (see Experimental section). Each of the Zn cations is tetrahedral coordinated by two terminal N-bonded thiocyanate anions and two 3-ethylpyridine ligands (Fig. 3). The Zn–N distances to the anionic ligands amount to 1.936(5)

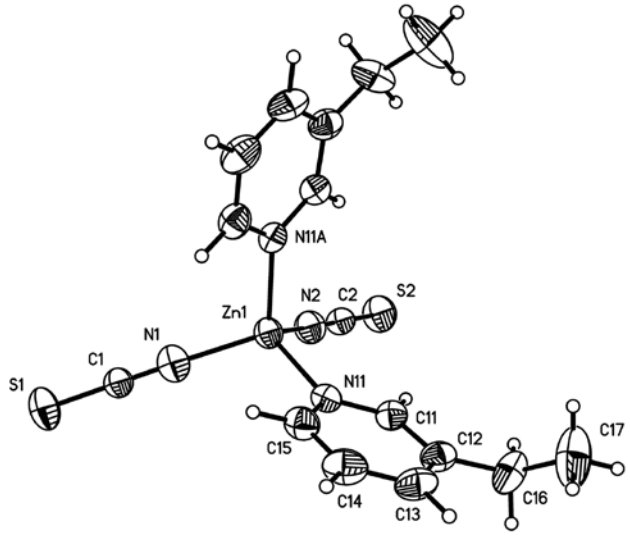

Fig. 3: Molecular structure of **2-Zn** with labeling and displacement ellipsoids drawn at the 50% probability level. Symmetry codes: A = –*x*, –*y*+1, –*z*+1.

and 1.949(5) Å and those to the neutral co-ligands are elongated to 2.027(3) Å.

Based on the single crystal data, X-ray powder diffraction (XRPD) patterns were calculated and compared with the experimental patterns, which show that **2-Cd** and **2-Zn** were obtained as pure phases, whereas **1-Zn** is always contaminated with small amounts of **2-Zn** (Fig. 4).

The reason why **1-Zn** is always contaminated with **2-Zn** can be traced back to the fact that **1-Zn** is unstable and transforms rapidly into the tetrahedral complex **2-Zn**, which obviously is more stable. The transformation is complete within several days as proven by XRPD (Fig. 5).

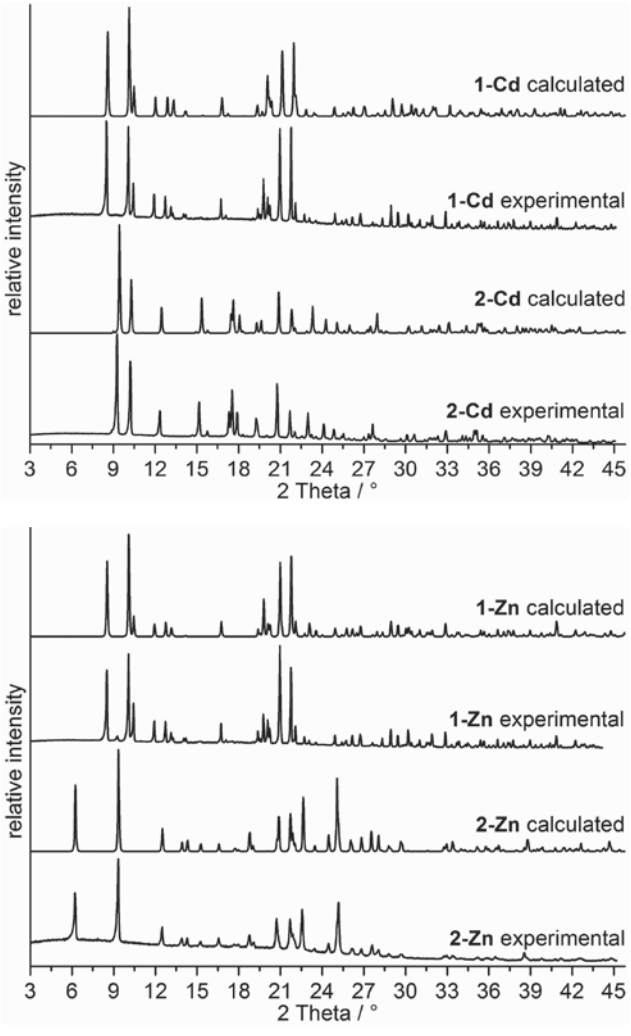

Fig. 4: Experimental and calculated XRPD pattern of the Cd (top) and the Zn compounds (bottom). It is noted, that the powder pattern for **1-Zn** was calculated using cell parameters retrieved from a Pawley Fit of a XRPD pattern measured at room temperature and that **1-Zn** is contaminated with a very small amount of **2-Zn**.

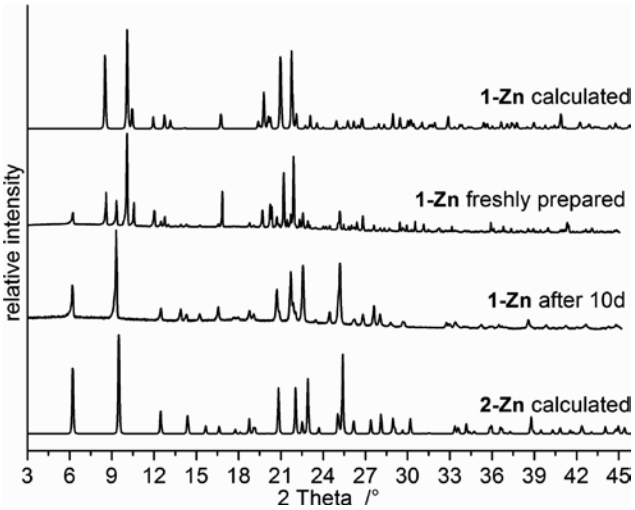

Fig. 5: Experimental XRPD pattern of freshly prepared **2-Zn** and after storage for 10 days as well as calculated XRPD pattern of **1-Zn** and **2-Zn**.

2.3 IR and Raman spectroscopic investigations

All compounds were investigated by IR and Raman spectroscopy to determine the value of the CN stretching vibration, which might be indicative for the coordination mode of the thiocyanate anion. For compound **1-Cd** this vibration is observed in the IR and in the Raman spectrum at 2054 cm^{-1}, which is in perfect agreement with values for terminally N-bonded thiocyanate anions retrieved from literature (Table 1) [27, 54].

In contrast, in **2-Cd** this band is shifted to 2086 cm^{-1}, which is below the threshold of about 2100 cm^{-1} expected for μ-1,3-bridging thiocyanate ligands [27]. For **1-Zn** the CN stretch is observed at 2068 and 2067 cm^{-1}, which is comparable to the values in **1-Cd** and in agreement with the fact that the CN stretching vibration for Zn is usually at higher values compared to Cd [27]. In agreement with the presence of terminal anionic ligands, for **2-Zn** the CN stretch is observed at 2067 and 2070 cm^{-1} (Table 2).

Table 1: Values of the CN stretching vibration (cm^{-1}) in the IR and Raman spectra of **1-Cd**, **2-Cd**, **1-Zn** and **2-Zn**.

Compound	IR	Raman
1-Cd	2054	2054
2-Cd	2086	2086
1-Zn	2068	2067
2-Zn	2067	2070

Table 2: Selected crystal data and details on the structure determinations for **1-Cd**, **1-Zn**, **2-Cd** and **2-Zn**.

	1-Cd	1-Zn	2-Cd	2-Zn
Formula	$C_{30}H_{36}N_6S_2Cd$	$C_{30}H_{28}N_6S_2Zn$	$C_{16}H_{18}N_4S_2Cd$	$C_{16}H_{18}N_4S_2Zn$
Mw, g mol^{-1}	657.17	602.07	442.86	395.83
Crystal system	triclinic	triclinic	triclinic	monoclinic
Space group	$P\bar{1}$	$P\bar{1}$	$P\bar{1}$	$P2_1/m$
a, Å	8.9530(7)	8.7995(3)	9.7549(7)	5.3291(3)
b, Å	9.2032(8)	9.1754(4)	10.4966(9)	12.3247(9)
c, Å	10.3365(11)	10.1918(4)	11.3560(8)	14.1835(9)
α, deg	87.784(12)	88.804(3)	96.712(9)	90
β, deg	83.895(11)	83.489(3)	114.763(8)	90.028(7)
γ, deg	71.153(10)	71.305(3)	110.364(9)	90
V, Å^3	801.45(14)	774.33(5)	941.58(15)	931.57(10)
T, K	200(2)	170(2)	200(2)	200(2)
Z	1	1	2	2
D_{calcd}, g cm^{-3}	1.36	1.29	1.56	1.41
μ, mm^{-1}	0.8	1.0	1.4	1.55
θ_{max}, deg	27.003	27.998	26.002	25.998
Refl. collected	6389	13 673	9649	6018
Unique refl.	3428	3743	3617	1905
R_{int}	0.0569	0.0281	0.0317	0.0460
Min/max transm.	0.787/0.932	0.703/0.913	0.718/0.791	–
Refl. [$F_0 > 4\,\sigma(F_0)$]	3143	3404	3034	1785
Parameters	178	178	243	117
R_1 [$F_0 > 4\,\sigma(F_0)$]	0.0288	0.0251	0.0309	0.0344
wR_2	0.0728	0.0660	0.0779	0.0846
GOF	1.062	1.057	1.030	1.076
$\Delta\rho_{max/min}$, *e* Å^{-3}	0.51/−0.83	0.28/−0.21	0.51/−0.64	0.33/−0.39

2.4 Thermoanalytical investigations

To check if compounds **1-Cd** and **1-Zn** can be transformed into **2-Cd**, respectively **2-Zn** or if different modifications are obtained, these compound were investigated by differential thermoanalysis (DTA) and thermogravimetry (TG). Upon heating at 1°C/min both compounds show one mass loss at about 104°C for **1-Cd**, respectively 51°C for **1-Zn**, which is accompanied with endothermic events in the DTA curve (Fig. 6: top). The experimental mass loss of 32.8% for **1-Cd** and of 33.8% for **1-Zn** is in reasonable agreement with that calculated for the removal of two 3-ethylpyridine ligands ($\Delta m_{calcd.} = 32.8\%$ for **1-Cd** and 35.2% for **1-Zn**). Therefore, one can assume that compounds with the composition $M(NCS)_2(3\text{-ethylpyridine})_4$ (M = Cd, Zn) are formed as intermediates. The low decomposition temperature also indicates that **1-Zn** is not very stable at room temperature. It is noted, that the decomposition temperatures are much lower than the boiling temperature of the 3-ethylpyridine ligand but it must be kept in mind, that the experiment was performed under dynamic conditions. In this case the gaseous ligand, which is in equilibrium with the solid, will be immediately removed leading to further decomposition. However, for some other discrete complexes built up of $Zn(NCS)_2$ melting is observed before the solid decomposes, but here we have no hint for such a scenario from microscopic investigations [51, 52]. On further heating the sample mass decreases continuously with no distinct mass steps, indicating the decomposition of the compound formed as an intermediate after the first mass loss. To identify the intermediate compounds the measurement was repeated, stopped after the first mass loss, and the residue was investigated by XRPD. Comparison of the experimental XRPD pattern with those calculated has shown, that **1-Cd** and **1-Zn** have been transformed into **2-Cd**, respectively **2-Zn** (Fig. 6: bottom).

2.5 Luminescence measurements

As shown in Figure 7, the compounds **1-Cd**, **2-Cd**, **2-Zn** and the 3-ethylpyridine ligand emit light in the blue spectral range. Specifically, the emission spectrum of **1-Cd** (Fig. 7, dashed curve, $\tilde{\nu}_{ex} = 25\,707$ cm^{-1}) consists of a broad band with a maximum at 21 724 cm^{-1} and full width at half maximum (FWHM) of 4748 cm^{-1}, strongly overlapping with the emission spectrum of **2-Cd** (Fig. 7, gray curve, $\tilde{\nu}_{ex} = 27\,027$ cm^{-1}) with a maximum at 21 654 cm^{-1} and FWHM of 4482 cm^{-1}.

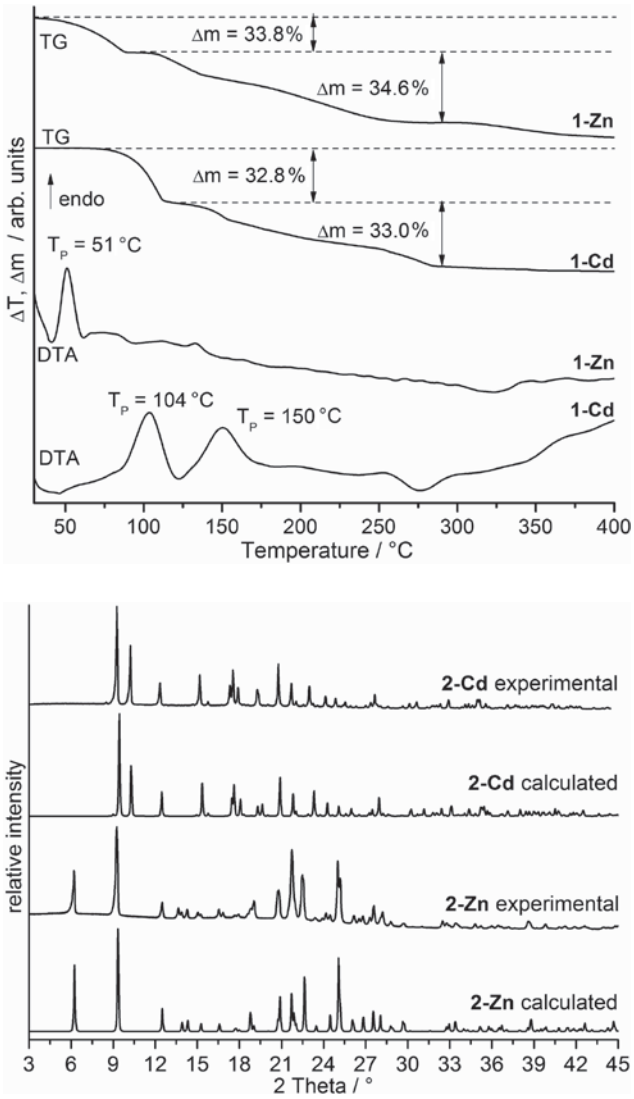

Fig. 6: DTA and TG curves of **1-Cd** and **1-Zn** measured at a heating rate of 1°C min^{-1} (top), and experimental XRPD patterns of the residues obtained after the first TG step together with the patterns calculated for **2-Cd** and **2-Zn** (bottom).

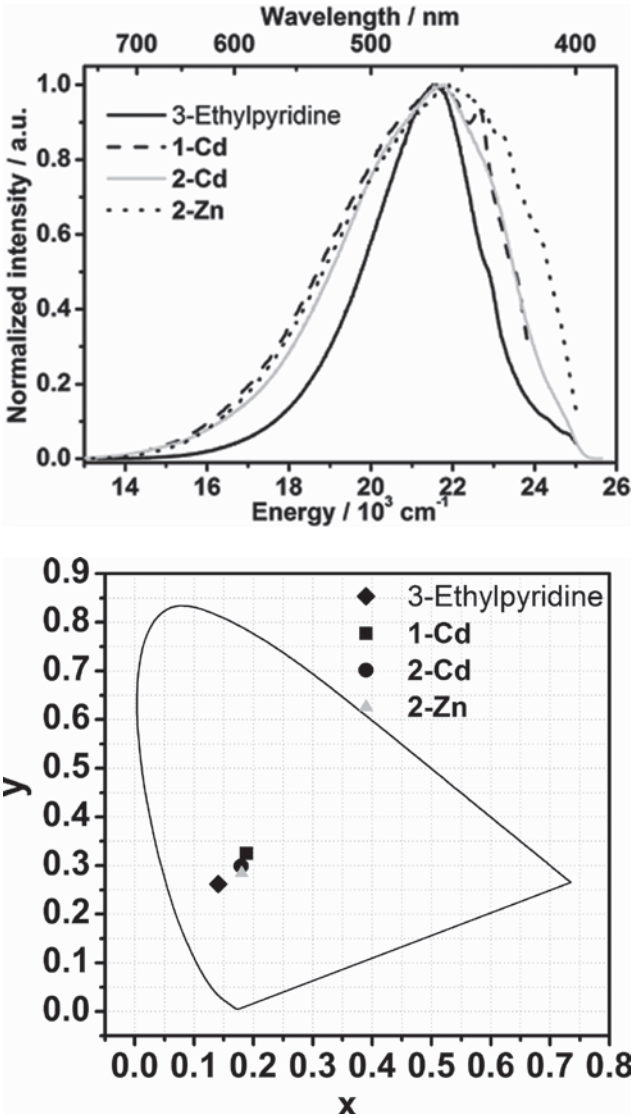

Fig. 7: Top: Emission spectra of the 3-ethylpyridine ligand (black curve, $\tilde{\nu}_{ex}$ = 25 294 cm^{-1}), **1-Cd** (dashed curve, $\tilde{\nu}_{ex}$ = 25 707 cm^{-1}), **2-Cd** (gray curve, $\tilde{\nu}_{ex}$ = 27 027 cm^{-1}), **2-Zn** (pointed curve, $\tilde{\nu}_{ex}$ = 26 316 cm^{-1}). Bottom: Plot of color coordinates on the CIE (Commission internationale de l'éclairage) 1931 chromaticity diagram for the 3-ethylpyridine ligand (♦), **1-Cd** (■), **2-Cd** (●) and **2-Zn** (▲).

Similarly, the emission spectrum of **2-Zn** (Fig. 7, pointed curve, $\tilde{\nu}_{ex}$ = 26 316 cm^{-1}) consists also of a broad band with a maximum at 22 055 cm^{-1} with FWHM of 5514 cm^{-1}.

The resemblance of these emission spectra for similar excitation energies is explained by the ligand-based nature of the optical properties. Since Cd^{2+} and Zn^{2+} do not present radiative electronic transitions, the optical properties of compounds **1-Cd**, **2-Cd** and **2-Zn** are based on the $S_1 \rightarrow S_0$ transition of the aromatic units within the organic ligand [55], as is also observed for other Cd^{2+}- and Zn^{2+}-based complexes, coordination polymers and metal-organic frameworks [44–47, 50–52, 56–58]. This fact is confirmed by the similarity of the emission spectra of **1-Cd**, **2-Cd** and **2-Zn** to that of the 3-ethylpyridine ligand (Fig. 7, solid black curve, $\tilde{\nu}_{ex}$ = 25 294 cm^{-1}), centered at 21 514 cm^{-1} with FWHM of 3106 cm^{-1}. Consequently, the resultant CIE 1931 color coordinates present also close values for **1-Cd** (x = 0.1879, y = 0.3254), **2-Cd** (x = 0.1794, y = 0.2988), **2-Zn** (x = 0.1802, y = 0.2846) and 3-ethylpyridine (x = 0.1407, y = 0.2619).

3 Conclusions

In the present contribution, new $Cd(NCS)_2$ and $Zn(NCS)_2$ coordination compounds with 3-ethylpyridine as co-ligand are reported. If an excess of 3-ethylpyridine is used in the

synthesis, discrete octahedral complexes with only terminally N-bonded anionic ligands are obtained. At lower metal salt to 3-ethylpyridine ratio, compounds of composition $M(NCS)_2$(3-ethylpyridine)$_2$ (M = Cd, Zn) are obtained, which in both cases can also be prepared by thermal decomposition of the 3-ethylpyridine rich precursor complexes. In the Cd compound the cations are octahedrally coordinated and linked into linear chains by the anionic ligands, which is a very common structure in this class of compounds. The corresponding Zn compound shows a tetrahedral coordination and therefore, this compound forms discrete complexes with still terminally N-bonded thiocyanate anions. The 3-ethylpyridine-rich compounds can be transformed into the 3-ethylpyridine deficient compounds by annealing, but the Zn compound **1-Zn** already transforms into **2-Zn** on storage at room-temperature, because for Zn the tetrahedral coordination is more stable. IR and Raman spectroscopic investigations have shown, that it is difficult for these compounds to distinguish the terminal and the bridging coordination modes of the anionic ligands. The emission spectra of **1-Cd**, **2-Cd**, **2-Zn** and the 3-ethylpyridine ligand show broad bands in the blue spectral range that originate from a ligand-based luminescence with no significant differences between the different compounds.

4 Experimental section

4.1 Synthesis

4.1.1 Syntheses of $Cd(NCS)_2$ and $Zn(NCS)_2$

$Ba(NCS)_2 \cdot 3H_2O$ and 3-ethylpyridine were obtained from Alfa Aesar and $ZnSO_4 \cdot H_2O$, $CdSO_4 \cdot 8/3H_2O$ were obtained from Merck. All chemicals were used without further purification. $Cd(NCS)_2$ and $Zn(NCS)_2$ were prepared by the reaction of equimolar amounts of $ZnSO_4 \cdot H_2O$, respectively $CdSO_4 \cdot 8/3H_2O$ and $Ba(NCS)_2 \cdot 3H_2O$ in water.

The resulting white precipitates of $BaSO_4$ were filtered off and the filtrate was concentrated to complete dryness resulting in white residues of $Zn(NCS)_2$ and $Cd(NCS)_2$. All crystalline powders were prepared by stirring of the reactants in solution for 3 days at room temperature. The residues were filtered off and washed with water and dried in air.

4.1.2 Syntheses of $Cd(NCS)_2$(3-ethylpyridine)$_4$ (1-Cd)

Single crystals suitable for X-ray structure determination were obtained by the reaction of $Cd(NCS)_2$ (34.3 mg, 0.15 mmol) with 3-ethylpyridine (68.3 µL, 0.60 mmol) in 2.5 mL H_2O in a closed test tube at room temperature for 3 days. A crystalline powder was obtained by the reaction of $Cd(NCS)_2$ (57.2 mg, 0.25 mmol) with 3-ethylpyridine (1.0 mL, 8.9 mmol). Elemental analysis for $C_{30}H_{36}CdN_6S_2$ (657.188 g mol^{-1}): C 54.83, H 5.52, N 12.79, S 9.76; found C 54.12, H 5.38, N 12.63, S 9.80.

4.1.3 Syntheses of $Cd(NCS)_2$(3-ethylpyridine)$_2$ (2-Cd)

Single crystals suitable for X-ray structure determination were obtained by the reaction of $Cd(NCS)_2$ (34.2 mg, 0.15 mmol) with 3-ethylpyridine (34.2 µL, 0.3 mmol) in 2.5 mL H_2O in a closed test tube for 3 days. A crystalline powder was obtained by the reaction of $Cd(NCS)_2$ (114.3 mg, 0.50 mmol) with 3-ethylpyridine (112.3 µL, 1.00 mmol) in 1.5 mL H_2O. Elemental analysis for $C_{16}H_{18}CdN_4S_2$ (442.8777 g mol^{-1}): C 43.39, H 4.1, N 12.65, S 14.48; found C 41.80, H 3.83, N 12.34, S 14.69.

4.1.4 Synthesis of $Zn(NCS)_2$(3-ethylpyridine)$_4$ (1-Zn)

Suitable single crystals for X-ray structure determination were obtained by the reaction of $Zn(NCS)_2$ (45.4 mg, 0.25 mmol) with 3-ethylpyridine (336.9 µL, 3.00 mmol) in 1.5 mL H_2O in a closed test tube at room temperature for five days. A phase pure polycrystalline powder was obtained through stirring $Zn(NCS)_2$ (0.5 mmol, 90.0 mg) in an excess of 3-ethylpyidine (17.8 mmol, 2.0 mL). It is noted that this compound transforms into **2-Zn** when stored at ambient conditions.

4.1.5 Synthesis of $Zn(NCS)_2$(3-ethylpyridine)$_2$ (2-Zn)

Suitable single crystals for X-ray structure determination were obtained by the reaction of $Zn(NCS)_2$ (54.4 mg, 0.30 mmol) with 3-ethylpyridine (34.2 µL, 0.30 mmol) in 1.0 mL ethanol in a closed test tube after 3 days. A crystalline powder was obtained by the reaction of $Zn(NCS)_2$ (90.8 mg, 0.50 mmol) with 3-ethylpyridine (112.3 µL, 1.00 mmol) in 1.5 mL H_2O. Elemental analysis for $C_{16}H_{18}N_4S_2Zn$ (395.8577 g mol^{-1}): C 48.55, H 4.58, N 14.15, S 16.20; found C 48.004, H 4.61, N 13.78, S 16.10.

4.2 Elemental analysis

CHNS analyses were performed using an EURO EA elemental analyzer, fabricated by EURO VECTOR Instruments.

4.3 Differential thermal analysis and thermogravimetry (DTA-TG)

DTA-TG measurements were performed in a dynamic nitrogen atmosphere in Al_2O_3 crucibles using a STA-PT1600 thermobalance from Linseis. The instrument was calibrated using standard references materials. All measurements were performed with a flow rate of 75 mL min^{-1} and were corrected for buoyancy.

4.4 X-ray powder diffraction (XRPD)

The measurements were performed using a stoe transmission powder diffraction system (STADI P) with $CuK_{\alpha1}$ radiation ($\lambda = 1.540\ 598$ Å) equipped with a MYTHEN 1K detector from STOE & Cie.

4.5 Single-crystal structure analyses

Data collections were performed with an imaging plate diffraction system IPDS-1 (**1-Cd**, **1-Zn**, **2-Cd** and **2-Zn**) and IPDS-2 (**2-Zn-H$_2$O**) from STOE & Cie using MoK_α radiation. Structure solutions were performed with Shelxt [59] and structure refinement was performed against F^2 using Shelxl-2014 [60]. A numerical absorption correction was applied using the programs X-Red and X-Shape of the program package X-Area [61–63]. All non-hydrogen atoms except the disordered C and N atoms of lower occupancy in **2-Cd** were refined with anisotropic displacement parameters. The hydrogen atoms were positioned with idealized geometry (methyl H atoms in **2-Zn** allowed to rotate but not to tip) and were refined isotropically with $U_{iso}(H) = -1.2\ U_{eq}(C)$ (1.5 for methyl H atoms) using a riding model. In **2-Cd** one of the ethyl groups of one crystallographically independent 3-ethylpyridine ligand as well as the other co-ligand are disordered and were refined using a split model. The lattice parameters of **2-Zn** indicate an orthorhombic crystal system but the crystal shows pseudo merohedral twinning, which is also indicated by a very low $|E \cdot E^{-1}|$ value of 0.584. Therefore a twin refinement was performed using the matrix ($\bar{1}\,0\,0,\ 0\,\bar{1}\,0,\ 0\,0\,1$) leading to a BASF parameter of 0.458(2). In an orthorhombic crystal system the systematic extinctions do not fit very well to any possible space group, but $P22_1$ or $P2_12_12$ might be acceptable. In these space groups an $Zn(NCS)_2$ fragment can be located, which is completely disordered around a two-fold rotation axis and a preliminary refinement always leads to inacceptable reliability factors, clearly indicating that the crystal symmetry is too high. Selected crystal data and details of the structure refinements can be found in Table 2.

CCDC 1585623 (**1-Cd**), 1585625 (**2-Cd**), 1585626 (**1-Zn**) and 1585624 (**2-Zn**) contain the supplementary crystallographic data for this paper. These data can be obtained free charge from the Cambridge Crystallographic Data Centre *via* http://www.ccdc.cam.ac.uk/data_request/cif.

4.6 IR and Raman spectroscopy

All IR data were obtained using an ATI Mattson Genesis Series FTIR Spectrometer, control software: Winfirst, from ATI Mattson. All Raman spectra were recorded using a IFS 66/CS NIR Fourier-Transform Raman spectrometer and a FRA 106 from Bruker.

4.7 Luminescence measurements

Luminescence spectra have been measured with a HORIBA Jobin Yvon GmbH (Unterhaching, Germany) spectrometer (Fluorolog3) at room temperature, equipped with an iHR-320-FA Triple Grating spectrograph, R928P Photomultiplier and a 450 W xenon lamp.

Acknowledgments: This project was supported by the Deutsche Forschungsgemeinschaft (Project No. Na 720/5-2 and TE1147/1-1) and the State of Schleswig-Holstein. We thank Prof. Dr. Wolfgang Bensch for access to his experimental facilities.

References

[1] A. J. Blake, N. R. Champness, P. Hubberstey, W.-S. Li, M. A. Withersby, M. Schröder, *Coord. Chem. Rev.* **1999**, *183*, 117.
[2] C. Janiak, L. Uehlin, H.-P. Wu, P. Klüfers, H. Piotrowski, T. G. Scharmann, *J. Chem. Soc., Dalton Trans.* **1999**, 3121.
[3] B. Moulton, M. J. Zaworotko, *Chem. Rev.* **2001**, *101*, 1629.
[4] S. L. James, *Chem. Soc. Rev.* **2003**, *32*, 276.
[5] C. Janiak, *Dalton Trans.* **2003**, 2781.
[6] L. Brammer, *Chem. Soc. Rev.* **2004**, *33*, 476.
[7] A. K. Bar, C. Pichon, J.-P. Sutter, *Coord. Chem. Rev.* **2016**, *308, Part 2*, 346.
[8] J. M. Clemente-Juan, E. Coronado, A. Gaita-Arino, *Chem. Soc. Rev.* **2012**, *41*, 7464.
[9] X. Y. Wang, C. Avendano, K. R. Dunbar, *Chem. Soc. Rev.* **2011**, *40*, 3213.
[10] S. Kitagawa, K. Uemura, *Chem. Soc. Rev.* **2005**, *34*, 109.
[11] A. H. Chughtai, N. Ahmad, H. A. Younus, A. Laypkov, F. Verpoort, *Chem. Soc. Rev.* **2015**, *44*, 6804.
[12] G. A. Craig, M. Murrie, *Chem. Soc. Rev.* **2015**, *44*, 2135.

[13] P. Silva, S. M. F. Vilela, J. P. C. Tome, F. A. Almeida Paz, *Chem. Soc. Rev.* **2015**, *44*, 6774.
[14] S. Dhers, H. L. C. Feltham, S. Brooker, *Coord. Chem. Rev.* **2015**, *296*, 24.
[15] B. Nowicka, M. Reczynski, M. Rams, W. Nitek, M. Koziel, B. Sieklucka, *CrystEngComm* **2015**, *17*, 3526.
[16] P. Konieczny, R. Pelka, D. Czernia, R. Podgajny, *Inorg. Chem.* **2017**, *56*, 11971.
[17] S. Suckert, M. Rams, M. M. Rams, C. Näther, *Inorg. Chem.* **2017**, *56*, 8007.
[18] M. Rams, Z. Tomkowicz, M. Böhme, W. Plass, S. Suckert, J. Werner, I. Jess, C. Näther, *Phys. Chem. Chem. Phys.* **2017**, *19*, 3232.
[19] S. Suckert, M. Rams, M. Böhme, L. S. Germann, R. E. Dinnebier, W. Plass, J. Werner, C. Näther, *Dalton Trans.* **2016**, *45*, 18190.
[20] S. Wöhlert, U. Ruschewitz, C. Näther, *Cryst. Growth Des.* **2012**, *12*, 2715.
[21] S. Wöhlert, T. Fic, Z. Tomkowicz, S. G. Ebbinghaus, M. Rams, W. Haase, C. Näther, *Inorg. Chem.* **2013**, *52*, 12947.
[22] S. Wöhlert, Z. Tomkowicz, M. Rams, S. G. Ebbinghaus, L. Fink, M. U. Schmidt, C. Näther, *Inorg. Chem.* **2014**, *53*, 8298.
[23] S. Wöhlert, M. Wriedt, T. Fic, Z. Tomkowicz, W. Haase, C. Näther, *Inorg. Chem.* **2013**, *52*, 1061.
[24] M. Rams, M. Böhme, V. Kataev, Y. Krupskaya, B. Büchner, W. Plass, T. Neumann, Z. Tomkowicz, C. Näther, *Phys. Chem. Chem. Phys.* **2017**, *19*, 24534.
[25] Y. P. Prananto, A. Urbatsch, B. Moubaraki, K. S. Murray, D. R. Turner, G. B. Deacon, R. Batten Stuart, *Aust. J. Chem.* **2017**, *70*, 516.
[26] A. Switlicka, K. Czerwinska, B. Machura, M. Penkala, A. Bienko, D. Bienko, W. Zierkiewicz, *CrystEngComm* **2016**, *18*, 9042.
[27] C. Näther, S. Wöhlert, J. Boeckmann, M. Wriedt, I. Jeß, *Z. Anorg. Allg. Chem.* **2013**, *639*, 2696.
[28] J. Werner, T. Runčevski, R. Dinnebier, S. G. Ebbinghaus, S. Suckert, C. Näther, *Eur. J. Inorg. Chem.* **2015**, 3236.
[29] J.-G. Uttecht, W. Preetz, *Z. Anorg. Allg. Chem.* **2001**, *627*, 1459.
[30] A. Tahli, J. K. Maclaren, I. Boldog, C. Janiak, *Inorg. Chim. Acta* **2011**, *374*, 506.
[31] M. A. S. Goher, F. A. Mautner, M. A. M. Abu-Youssef, A. K. Hafez, A. M. A. Badr, C. Gspan, *Polyhedron* **2003**, *22*, 3137.
[32] B. Machura, A. Świtlicka, J. Mroziński, B. Kalińska, R. Kruszynski, *Polyhedron* **2013**, *52*, 1276.
[33] J. L. Guillet, I. Bhowmick, M. P. Shores, C. J. A. Daley, M. Gembicky, J. A. Golen, A. L. Rheingold, L. H. Doerrer, *Inorg. Chem.* **2016**, *55*, 8099.
[34] J. Palion-Gazda, B. Machura, F. Lloret, M. Julve, *Cryst. Growth Des.* **2015**, *15*, 2380.
[35] R. González, A. Acosta, R. Chiozzone, C. Kremer, D. Armentano, G. De Munno, M. Julve, F. Lloret, J. Faus, *Inorg. Chem.* **2012**, *51*, 5737.
[36] E. Shurdha, C. E. Moore, A. L. Rheingold, S. H. Lapidus, P. W. Stephens, A. M. Arif, J. S. Miller, *Inorg. Chem.* **2013**, *52*, 10583.
[37] E. Shurdha, S. H. Lapidus, P. W. Stephens, C. E. Moore, A. L. Rheingold, J. S. Miller, *Inorg. Chem.* **2012**, *51*, 9655.
[38] M. Mousavi, V. Bereau, C. Duhayon, P. Guionneau, J.-P. Sutter, *Chem. Commun.* **2012**, *48*, 10028.
[39] B. Machura, A. Świtlicka, I. Nawrot, J. Mroziński, R. Kruszynski, *Polyhedron* **2011**, *30*, 832.
[40] S. Suckert, M. Rams, L. Germann, D. M. Cegiełka, R. E. Dinnebier, C. Näther, *Cryst. Growth Des.* **2017**, *17*, 3997.
[41] J. Werner, M. Rams, Z. Tomkowicz, T. Runčevski, R. E. Dinnebier, S. Suckert, C. Näther, *Inorg. Chem.* **2015**, *54*, 2893.
[42] S. Wöhlert, L. Peters, C. Näther, *Dalton Trans.* **2013**, *42*, 10746.
[43] S. Wöhlert, I. Jess, U. Englert, C. Näther, *CrystEngComm* **2013**, *15*, 5326.
[44] F. A. Mautner, C. Berger, R. C. Fischer, S. S. Massoud, *Inorg. Chim. Acta* **2016**, *439*, 69.
[45] F. A. Mautner, C. Berger, R. C. Fischer, S. S. Massoud, *Polyhedron* **2016**, *111*, 86.
[46] F. A. Mautner, C. Berger, R. C. Fischer, S. S. Massoud, *Inorg. Chim. Acta* **2016**, *448*, 34.
[47] F. A. Mautner, M. Scherzer, C. Berger, R. C. Fischer, S. S. Massoud, *Inorg. Chim. Acta* **2015**, *425*, 46.
[48] I. Nawrot, B. Machura, R. Kruszynski, *CrystEngComm* **2016**, *18*, 2650.
[49] D.-B. Dang, X.-F. Hu, Y. Bai, Z.-Y. Qi, F. Yang, *Inorg. Chim. Acta* **2011**, *377*, 20.
[50] S. Suckert, H. Terraschke, H. Reinsch, C. Näther, *Inorg. Chim. Acta* **2017**, *461*, 290.
[51] T. Neumann, C. dos Santos Cunha, H. Terraschke, L. S. Germann, R. E. Dinnebier, I. Jess, C. Näther, *Z. Anorg. Allg. Chem.* **2017**, *643*, 1497.
[52] T. Neumann, L. S. Germann, I. Moudrakovski, R. E. Dinnebier, C. Dos Santos Cunha, H. Terraschke, C. Näther, *Z. Anorg. Allg. Chem.* **2017**, *643*, 1904.
[53] E. Ďurčanská, M. Jamnický, M. Koman, I. Wnęk, T. Głowiak, *Acta Crystallogr.* **1986**, *C42*, 1157.
[54] R. A. Bailey, S. L. Kozak, T. W. Michelsen, W. N. Mills, *Coord. Chem. Rev.* **1971**, *6*, 407.
[55] W. W. Lestari, P. Lönnecke, H. C. Streit, M. Handke, C. Wickleder, E. Hey-Hawkins, *Eur. J. Inorg. Chem.* **2014**, *2014*, 1775.
[56] W. W. Lestari, H. C. Streit, P. Lonnecke, C. Wickleder, E. Hey-Hawkins, *Dalton Trans.* **2014**, *43*, 8188.
[57] W. W. Lestari, P. Lonnecke, M. B. Sarosi, H. C. Streit, M. Adlung, C. Wickleder, M. Handke, W.-D. Einicke, R. Glaser, E. Hey-Hawkins, *CrystEngComm* **2013**, *15*, 3874.
[58] C. Näther, I. Jess, L. S. Germann, R. E. Dinnebier, M. Braun, H. Terraschke, *Eur. J. Inorg. Chem.* **2017**, 1245.
[59] G. M. Sheldrick, *Acta Crystallogr.* **2015**, *A71*, 3.
[60] G. M. Sheldrick, *Acta Crystallogr.* **2015**, *C71*, 3.
[61] X-Red (version 1.11), Program for Data Reduction and Absorption Correction, STOE & Cie GmbH, Darmstadt (Germany), **1998**.
[62] X-Shape, (version 1.03), Program for the Crystal Optimization for Numerical Absorption Correction, STOE & Cie GmbH, Darmstadt (Germany), **1998**.
[63] X-Area (version 1.44), Program Package for Single Crystal Measurements, STOE & Cie GmbH, Darmstadt (Germany), **2008**.